COMPUTATIONAL AND EXPERIMENTAL STUDIES ON MOTION OF YIELD STRESS PLUGS IN CHANNELS

Parsa Zamankhan[*], Yingying Hu[*], Cheng-Feng Tai[*], Marcel Filoche[*,**], John C. Grotberg[***], Shiyao Bian[*], Shuichi Takayama[*], James B. Grotberg[*a)]

[*]*Department of Biomedical Engineering, University of Michigan, Ann Arbor, MI 48109, USA*

[**]*Physique de la Matière Condensée, Ecole Polytechnique, CNRS, 91128 Palaiseau, France*

[***]*University of Illinois at Chicago, Chicago, IL 60607, USA*

Summary We numerically and experimentally studied the propagation of liquid plugs with yield stress in channels in order to understand the mechanisms relevant to re-opening of occluded airways by mucus plugs. The computational and experimental results show that a yield stress in the biological range significantly increases the required driving pressure and induced wall shear stress level during the re-opening procedure. These indicate that the yield stress property of mucus can enhance the chance of the epithelial cell injuries in re-opening of blocked airways.

INTODUCTION

Mucus plugs are formed in the lung under a variety of circumstances including disease states which cause an excess of liquid there, or reductions of surfactant activity which increases the surface tension. As a result, they block the gas exchange in some sections of the lung. The reopening process involves propagation and rupture of these plugs. In this paper which is a continuation of one of our previous studies [1], the re-opening of occluded airways is investigated through simulations and experiments. In the numerical part, the transient motion of a liquid plug in a liquid coated 2D channel is investigated. Mucus is a non-Newtonian fluid with a yield stress which we assume is a Bingham fluid in this work. Through a parametric study, we determine the required driving pressure for initiation of the motion, the motion of the plug under larger driving pressure, the plug shape, the velocity and stress fields and from them the wall stresses. In the experimental part, aqueous Carbopol 940 (C940) at four concentrations is used as a mucus simulant with a yield stress and shear thinning properties. A small collapsed airway is simulated in a 2D polydimethylsiloxane (PDMS) channel. A syringe pump is used to compress atmospheric gas upstream of a Carbopol plug to drive its motion. A high-speed camera and particle image velocimetry technique are used to acquire images and velocity fields during the process of plug propagation and rupture. In the experiment, we also measure the critical pressure drop needed for a plug to rupture and wall stresses which, in a lung, would be transferred to epithelial cells of the airways.

METHODOLOGY OF COMPUTATIONAL FLUID DYNAMICS

We assume mucus as a Bingham fluid. In the Bingham fluid model for von Mises stresses less than a threshold yield stress, the medium undertakes no deformation similar to rigid solids. For von Mises stresses greater than the yield stress the medium behaves such as a Newtonian fluid. To ease the numerical simulations we use a regularized method as an approximation for the Bingham fluid model. Figure 1 shows the initial shape of a plug including two semi-circles attached to two horizontal lines. We assume that the driving pressure difference across the two menisci is constant and the thickness of the pre-cursor film, H_1, remains unchanged. We scale the length dimensions by b, velocity by σ/μ_p, pressure and stresses by σ/b and time by $b\mu_p/\sigma$, where b is the half width of the channel, σ is the gas-liquid surface tension, and μ_p is the plastic viscosity. The governing equations in dimensionless form then are:

Mass: $\nabla\cdot\vec{V}=0$ (1),

Momentum: $\lambda\left(\partial\vec{V}/\partial t+\left(\vec{V}\cdot\nabla\right)\vec{V}\right)=-\nabla p+\nabla\cdot\left(\eta\left(\nabla\vec{V}+\left(\nabla\vec{V}\right)^T\right)\right)$ (2)

Where $\eta=1+\left(1-\exp\left(-m\dot{\gamma}\right)\right)\ \tau_{yd}/\dot{\gamma}$ (3), $\lambda=\mathrm{Re}/Ca=\rho\sigma b/\mu_p^{\,2}$ (4), $\tau_{yd}(Bn\times Ca)=\tau_y/(\sigma/b)$ (5). At the out flow and wall: u=v=0 while at the inflow u=0. At the centerline: $\partial u/\partial y=0, v=0$. The boundary conditions at the free surfaces are: Kinematic: $(\vec{V}-\dot{X})\cdot\vec{n}=0$ (6), Stress: $-p\vec{n}+\eta(\nabla\vec{V}+(\nabla\vec{V})^T)\cdot\vec{n}=\kappa\vec{n}-p_i\vec{n}\ (i=1,2)$ (7). The precursor film thickness, H_1, is an input which assumed to be fixed in this study. We used a finite element formulation embedded with an ALE method to resolve the free surface.

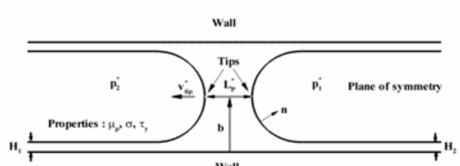

Fig.1: A scheme of a Bingham fluid plug to model mucus.

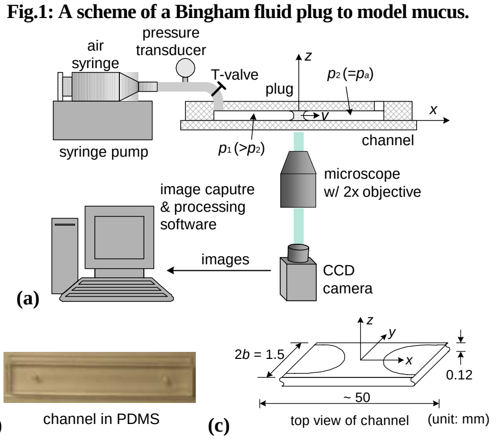

Fig.2: (a) Experiment to simulate mucus plug dynamics in a collapsed small airway. (b) The 2D channel in PDMS. (c) The channel dimensions, b=half channel width.

METHODOLOGY OF THE EXPERIMENTS

The mucus simulant, aqueous C940, is neutralized by 18% aqueous sodium hydroxide to acquire a clear gel with yield stress and shear thinning. The gel concentration varies from 0.1%, 0.15%, 0.2% to 0.3%. Their shear rate and shear stress follow the Herschel-Bulkley model. Yield stress increases with gel concentration. The 0.2% gel with yield stress of 510 dyne/cm^2 is comparable to normal human lung mucus. Figure 2 shows a 2D channel used to simulate a collapsed small lung airway as is found in the generations 9-12, for example. The pressure drop rises by a step increment until the plug ruptures. The channel with

a) corresponding author. Email: grotberg@umich.edu.

the plug is mounted on a microscope platform. A CCD camera is connected to a 2x objective lens to capture rupture images at a speed of 27.96 frames per second. The images are processed in an image software package, from which velocity vectors are calculated using PIV processing software. All experiments are done in a normal room condition.

RESULTS AND DISCUSSIONS

Computational Fluid Dynamics: We performed our simulations for a small airway of an average adult person where b=1.125 mm for a trachea of 1.8 cm according to Weibel model [2]. We used the following set of properties for mucus [3], ρ=1 g/cm^3, μ_p=1 poise, σ=80 dyne/cm, τ_y=400-800 dyne/cm^2. The initial plug length and the precursor film thickness are 1.125mm and 0.2 mm respectively. Figure 3 shows the time average of the plug speed for different driving pressure and different yield stress. For each value of the yield stress there is a critical driving pressure for the initiation of the motion. Figure 4a, however, shows that this driving pressure might not be adequate for the continuation of the motion as the plug speed initially increases but then it decreases until the plug stops. This is due to evolution of the plug shape to another configuration requiring a larger driving pressure for the initiation of the motion. We increased the driving pressure nearly 5 times leading to a motion with acceleration depicted in Figure 4b. For this case the trailing meniscus moves faster than the leading one indicating that the plug length becomes shorter during the motion and would rupture.

Figure 5 a-c shows the plug shape moving under a driving pressure of 7900 dyne/cm^2. For this case the plug undertakes significant deformation during the translation. The examination of the data shows that the plug becomes 2.5% shorter after 0.002 s. The bottom half of each figure shows the von Mises stress where the white regions are un-yielded. The examination of data showed that for this case that the wall shear stress level increases significantly during the motion owing the plug accleration.

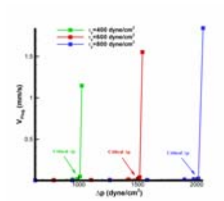

Fig.3: Plug speed in term of driving pressure.

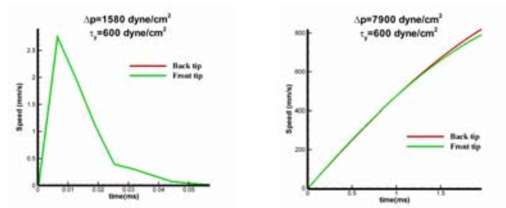

(a) **(b)**

Fig.4: Plug speed versus time for different driving pressure.

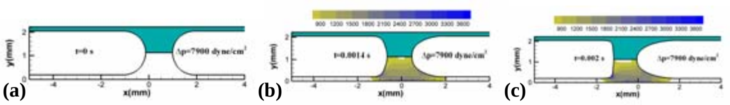

(a) **(b)** **(c)**

Fig.5: The plug shape during the motion.

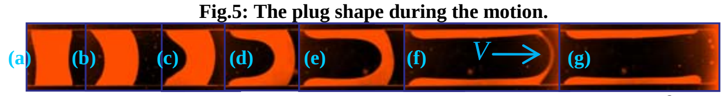

Fig.6: The plug deformation and rupture at L_{p0}=1.15, Δp=8027 dyne/cm^2 and gel concentration of 0.1%. (a) T_0 (the moment when Δp is imposed), (b) T_0+3.22s, (c) -4.51s (>T_0+3.22s), (d) -0.57s, (e) -0.21s, (f) 0 (rupture moment), and (g) 0.036s.

Experiments: Scaled on b, the dimensionless initial plug length is L_{p0}. Figure 6 shows the rupture process of a 0.1% gel plug at L_{p0}=1.15 and Δp=8027dyne/cm^2. The plug first propagates a distance in the channel, and then yields until ruptures (with droplet deposit). The critical pressure drop, Δp, that leads to eventual rupture was measured for varying L_{p0} and repeated for the four C940 concentrations. The experiments show that Δp increases with increasing L_{p0} in Fig. 7. At the same L_{p0} value, the plug at higher concentration needs a higher Δp to rupture. Figure 8 shows the features of wall shear stress and its gradient along the bottom channel wall at t=-0.179s. Wall shear stress was calculated from velocity vector fields processed through the PIV technique, using the Herschel-Bulkley model. Wall shear stress reaches its peak value around the plug and then rapidly returns to zero. The wall shear stress gradient has its maximum during the sharp change of wall shear stress returning to zero from its peak.

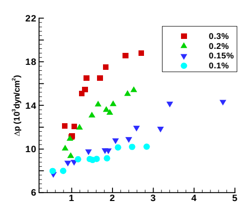

Fig.7: The critical pressure drop increases with L_{p0} and gel concentration.

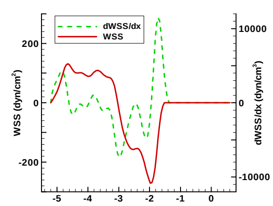

Fig.8: Wall shear stress (WSS) and its gradient (dWSS/dx) at L_{p0}=1.15, Δp=8027 dyn/cm^2 and gel concentration of 0.1%. x=0 (scaled by b) is the plug tip position at the rupture moment.

CONCLUSIONS

We studied the transient propgation of yield stress liquid plugs in CFD and experiments in order to understand the involved processes of reopening of occluded airways by mucus. For plugs with an initial shape as semi-circle there is a critical driving pressure for initiation of the motion. This driving pressure however leads to evolution of the plug shape rather than the translation and rupture. Siginificant increase in the driving pressure leads to a motion with accleration where the plug length decreases during the motion. For this regime the amplitude of the wall shear stress increases significantly owing to the accleration. The critical driving pressure increases with both initial length and yield stress of the plug.

ACKNOWLEDGMENTS

We thank NIH for supporting this work through the grants HL84370, and HL85156.

References

[1] P.Zamankhan, B.T. Helenbrook, S. Takayama, J. B. Grotberg, J. Fluid Mech., doi:10.1017/jfm.2011.438.
[2] E. R. Weibel, Morphometry on the Human Lung, Academic press, 1963.
[3] A.Bush, D. Payne, S. Pike, G. Jenkins,M.O. Henke, and B. K. Rubin, Chest 129(1),118-123, 2006.